Cooperation of Peripheral Hydrogen Atoms for the Stabilization of *Aachno*-pentaborane (11) with Small Molecules: Hydrogen Bonds and Dihydrogen Bonds

M. M. Salehnassaj [a], M. Nikorazma [a], A. Zabardasti [b], H. Goudarziafshar [c], and Boaz G. Oliveira* [d]

Post-Hartree-Fock calculations performed at the MP2/aug-cc-pVDZ level of theory has been used to analyze the formation of intermolecular complexes between B_5H_{11} and W = CO, NCH, NH_3, H_2O or $HOCH_3$. The interactions on the structure of the *arachno*-pentaborane(11) are manifested by the terminal and bridge hydrogen atoms, whereby are formed the hydrogen bonds (H···Y with Y = O, C or N) as well as dihydrogen bonds (H···H). In this context, the B_5H_{11} shows a host-guest capability for trapping molecules, of course depending on the strength of each aforementioned interactions. The topological descriptors of the Quantum Theory of Atoms in Molecules (QTAIM) were decisive for unveiling each one of the following structures B_5H_{11}···CO, B_5H_{11}···NCH, B_5H_{11}···NH_3, B_5H_{11}···H_2O and B5H₁₁···$HOCH_3$, and ideally, all hydrogen bonding formed by them.

Graphical abstract
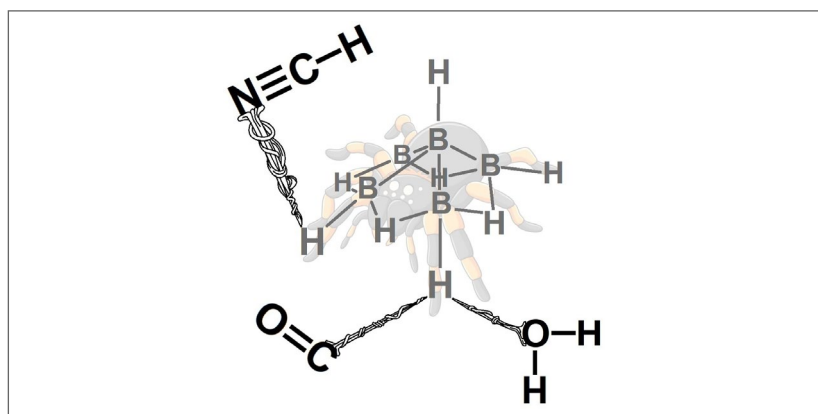
1. Introduction

In the last few years, the chemistry of the intermolecular interactions [1-3] has expanded its horizons beyond the traditional research of small bound complexes [4-5], wherein the studies involving highly-complexity systems have become a real challenge [6-8]. Specifically, with regards to the conceptions of hydrogen bonds [9], the historical knowledge concerning to the criterion of the lone pairs of valence electrons of oxygen, fluorine, sulfur and nitrogen compose the foundation of most of the intermolecular interactions [10]. Even this standard model being often observed in organic

[a] Department of Chemistry, Faculty of Science, Ilam University, Ilam, Iran. [b] Department of Chemistry, Faculty of Science, Lorestan University, Khorramabad, Iran. [c] Department of Chemical Engineering, Hamedan University of Technology, Hamedan, Iran. [d] Universidade Federal Do Oeste da Bahia, Centro das Ciências Exatas e das Tecnologias, Barreiras, Brazil. *Corresponding author. E-mail: **boazgaldino@gmail.com**

molecules, truly it is not unanimous because the electron density belonging to the π clouds of hydrocarbons also function as proton receptors to form hydrogen bonds [11-12]. In inorganic chemistry, however, the bulwark of the intermolecular contacts regarding the intermediate role of the hydrogen bond is also widely known among the chemists, physicists, biologists from all over the world [13-14]. Among many cases, the researches of borane clusters [15] conducted by Brown led him to be laureate with the Noble Prize in Chemistry 1979 [16], although this same honor has already been awarded to Lipscomb two years before [17]. In a brief comment about the researches of weakly bound systems, we can cite a derivative from the borane known as *arachno*-pentaborane(11), B_5H_{11}, which even though has a highly complex structure, its capability in forming intermolecular systems with small molecules has been elucidated [18].

Besides the standard hydrogen bonding profiles exhibited in the forms of O···H, N···H and F···H [19], recent works are emphatic in affirming that dihydrogen bonds H···H [20] as well as the lithium bonds Li···H [21] belong to the select group of interactions with significant role in many branches of the science. Nevertheless, concerning the dihydrogen bonds, for instance, some of its particularities are quite similar to those of traditional hydrogen bonds [22-23], e.g., the trend in occurring as a bifurcated interaction or directional one. In furtherance, the vibrational modes active in the infrared spectrum also shall provide systematic tendencies of interaction strength. As a matter of fact, based in the knowledge of the properties of the B_5H_{11}···X complexes (X = HF, LiH, O_2 and N_2) [24-25], the planning of our theoretical study aimed to identify which kinds of interactions must exist among B_5H_{11} and CO, NCH, H_2O, NH_3 or $HOCH_3$, and obviously, once possible, a parallelism to that is known about similar complexes, or even others bound systems, truly we are convinced that a contribution to the knowledge of the intermolecular studies carried so far must be reported here. In other words, this kind of intermolecular study unveils the main characteristic of host-guest in B_5H_{11}, and thereby it becomes one more goal to be examined here.

Once the diversity of computational methodologies used in studies of intermolecular systems has been widely established [26], the carrying out of this work was feasible through a carefully chosen of the most suitable theoretical level. Throughout the years, the development of the *ab initio* computational approaches and density functional theory functionals was planned in order to explore the electronic structure [27], and also, the properties and parameters either from spectroscopic nature or those related to the structure of intermolecular weakly bound complexes [28]. Here, we elected the sophisticated MP2/aug-cc-pVDZ theoretical level due to its efficiency and accuracy in studies of systems formed by borane and derivatives [29]. Furthermore, in recent decades, the phenomenology of the electronic structure has been intrinsically unveiled at the atomic level ruled by the exchange of charge and momentum between atoms that share electronic density [30]. It was by this criterion that Bader proposed the Quantum Theory of Atoms in Molecules (QTAIM) [31], wherein, throughout all of these years it has been considered a suitable vision of the electronic structure beyond the atoms in molecules. As far as the intermolecular studies of weakly bound complexes, the protocol of the QTAIM approach is fundamental to locate Bond Critical Points (BCPs) along the Bond Paths (BPs), i.e., an atomic frontier between two atoms often represented by an acid and base of Lewis, for instance.

The routine of the QTAIM calculations consists in measuring of the charge density (ρ) followed by computation of its Laplacian ($\nabla^2\rho$). This pair of descriptors composes a qualitative diagnose of interaction strength, which can be a covalent bond or even a weak intermolecular interaction [32-33]. Moreover, the overlapping of the frontier molecular orbital plays a decisive role for comprehending the formation of hydrogen bonds, and as such, the atomic charge calculation becomes indispensable to estimate the intermolecular charge transfer. This procedure should be performed by means of the atomic charge variations after the formation of the complex. Even though the determination of the total charge transfer amounts is not allowed for some specific systems [34-35], there is no deterrent for determining the variations of punctual atomic charge. In an overview, it will be through the MP2/aug-cc-pVDZ theoretical level that structural parameters, electronic properties, QTAIM integrations and NBO analyses, by which, in practice, the charge transfers, infrared vibration modes as stretching frequencies and absorption intensities of the B_5H_{11}···W (W = CO, NCH, NH_3, H_2O or $HOCH_3$) complexes, all these sorts of analyses encompass the scope of this current work.

2. Material and Methods

2.1 Computational methods

The geometries of the B5H11, CO, NCH, NH_3, H_2O and $HOCH_3$ monomers and consequently of the complexes of B_5H_{11}···CO, B_5H_{11}···NCH, B_5H_{11}···H_2O, B_5H_{11}···NH_3 and B_5H_{11}···$HOCH_3$ were fully optimized at the MP2/aug-cc-pVDZ computational level with all calculations carried out by the GAUSSIAN 09 program [36]. No imaginary frequency was observed in the infrared spectra with all structures optimized as minima along the potential energy surface. In view of this, the values of the Zero-Point vibrational Energies (ZPE) were then taken into account for correction of the intermolecular energies [37]. In addition, the function of Boys and Bernardi's counterpoise was also applied in this correction following the procedure of the Basis Set Superposition Error (BSSE) [38]. The AIM2000 package [39] was used to obtain the topological properties in according with the QTAIM formalism

3. Results and Discussion

Structures and infrared spectra

The optimized geometries of the B_5H_{11}···CO (**I**), B_5H_{11}···NCH (**II**), B_5H_{11}···H_2O (**III**), B_5H_{11}···NH_3 (**IV**) and B_5H_{11}···$HOCH_3$ (**V**) complexes are illustrated in Fig. 1. Based on the MP2/aug-cc-pVDZ calculations, the values of bond lengths are listed in Table 1. Firstly, the interaction strength may be explored through the intermolecular distances. In an overview, the intermolecular complexes with shorter hydrogen bond lengths are formed by H_2O (2.3944 Å), NH_3 (2.7043 Å) and $HOCH_3$ (2.5604 Å) while the longest ones interact with CO (2.9810 Å) and NCH (2.6393 Å). By taking into account the shorter distances of 2.7043 and 2.6393 Å, it may be claimed that the preferred hydrogen bond in **II** and **IV** is N···H^b−B. Nevertheless, the most likely hydrogen bond in **III** and **V** is O···H−B because the lone-electron pairs of oxygen interact simultaneously with both of H^a and H^b atoms, whereby the interactions lengths are 2.3944 and 2.5604 Å, respectively.

Among the **III**, **IV** and **V** supermolecules, their shorter interaction lengths occur upon the formation of dihydrogen bonds (H···H^d−B), whose values are 2.3944, 2.5775 and 2.3563 Å, respectively. Besides the four-center interactions

[40], it is important to notice that H_2O, NH_3 and $HOCH_3$ behave like amphoteric molecules, and for this reason, multiple interactions are formed on B_5H_{11}. However, it must be highlighted that not all protonic centers (OH and NH) are direct participant in the interaction process. Regarding the lengths of rW', we can mention the C−H bond of NCH, whose value of 1.0783 Å undergoes a slight variation of -0.0002 Å in comparison with the result of 1.0781 Å in **II**. For the length of O−H, the value of 0.9658 Å for the H_2O monomer increases slightly in 0.0003 Å whether compared with the value of 0.9661 Å in **III**. Finally, the enhancement of 0.0006 Å was determined by the subtraction between the values of 1.0204 (monomer) and 1.0210 Å (complex), and actually this result indicates that N−H is the bond more affected. In **V**, however, the C−H variation of 0.0006 Å is precisely the same value of **IV**. About the intermolecular interactions, certain deformations on molecular structure are expected usually occurring in the proton donors [41].

Still in according with the values listed in Table 1, it may be established a systematic trend in the bond length variations of CO, NCH, NH_3, H_2O and $HOCH_3$, although regardless the CO and NCH molecules, mainly the latter one, behave as proton receptors instead of donors like the other ones. Once this reasoning is feasible in traditional studies of weakly bound systems [42-43], the relative strength of hydrogen bonds in the $B_5H_{11}\cdots W$ complexes can be fairly attributed to the variations of their rW bonds, whose values are -0.0006, -0.0006, 0.0015, 0.0009 and 0.0016 Å. However, the bond lengths in the **I** and **II** complexes were shortened, although the increase is an inherent characteristic in **III**, **IV** and **V**. Specifically in B_5H_{11}, a

certain synchronism can be observed in the variations of the B−H bonds, mainly the shortening of both $B^1−H^a$ and $B^3−H^b$. In opposition to this, the $B^2−H^b$ and $B^4−H^c$ bonds exhibit indistinct systematic tendencies, i.e., reductions in **II** and **IV** followed by increase in **I**, **III** and **V**. Singly, the $B^2−H^a$ bond length is enhanced in all complexes. Briefly commenting, it must be emphasized that no relationship between the intermolecular distances and the variations of bond lengths of B_5H_{11} and CO, NCH, H_2O, NH_3 and $HOCH_3$ was observed.
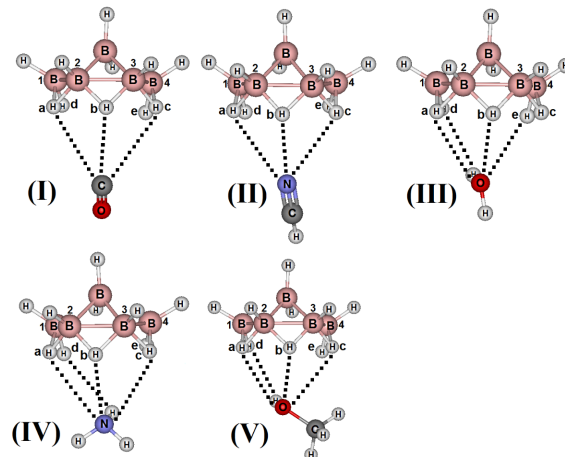

Fig. 1. Optimized geometries of the $B_5H_{11}\cdots CO$ (**I**), $B_5H_{11}\cdots NCH$ (**II**), $B_5H_{11}\cdots H_2O$ (**III**), $B_5H_{11}\cdots NH_3$ (**IV**) and $B_5H_{11}\cdots HOCH_3$ (**V**) complexes obtained through the MP2/aug-cc-pVDZ theoretical level.

Table 1. Bond lengths (Å) of the $B_5H_{11}\cdots CO$ (**I**), $B_5H_{11}\cdots NCH$ (**II**), $B_5H_{11}\cdots H_2O$ (**III**), $B_5H_{11}\cdots NH_3$ (**IV**) and $B_5H_{11}\cdots HOCH_3$ (**V**) complexes obtained at the MP2/aug-cc-pVDZ level of theory.

Bonds	Complexes				
	I	II	III	IV	V
$R_{(C\cdots H^a-B)}$	3.0514	−	−	−	−
$R_{(C\cdots H^b-B)}$	2.9810	−	−	−	−
$R_{(C\cdots H^c-B)}$	3.1455	−	−	−	−
$R_{(N\cdots H^a-B)}$	−	2.9322	−	2.9830	−
$R_{(N\cdots H^b-B)}$	−	2.6393	−	2.7043	−
$R_{(N\cdots H^c-B)}$	−	2.8315	−	2.8911	−
$R_{(O\cdots H^a-B)}$	−	−	2.3944	−	2.6782
$R_{(O\cdots H^b-B)}$	−	−	2.5865	−	2.5604
$R_{(O\cdots H^c-B)}$	−	−	2.9416	−	2.8668
$R_{(H\cdots H^d-B)}$	−	−	2.3944	2.5775	2.3563
r_W	1.1496 (1.1502) [-0.0006]	1.1822 (1.1828) [-0.0006]	0.9673 (0.9658) [0.0015]	1.0213 (1.0204) [0.0009]	0.9674 (0.9658) [0.0016]
$r_{W'}$	− (−) [−]	1.0781 (1.0783) [-0.0002]	0.9661 (0.9658) [0.0003]	1.0210 (1.0204) [0.0006]	1.1035 (1.1029) [0.0006]
$r_{B^1-H^a}$	1.3916 (1.4119) [-0.0203]	1.4053 (1.4119) [-0.0066]	1.3872 (1.4119) [-0.0247]	1.4039 (1.4119) [-0.0080]	1.3869 (1.4119) [-0.0250]
$r_{B^2-H^a}$	1.2907 (1.2745) [0.0162]	1.2764 (1.2745) [0.0019]	1.2919 (1.2745) [0.0174]	1.2756 (1.2745) [0.0011]	1.2919 (1.2745) [0.0174]
$r_{B^2-H^b}$	1.3631 (1.3311) [0.0320]	1.3269 (1.3311) [-0.0042]	1.3608 (1.3311) [0.0297]	1.3277 (1.3311) [-0.0034]	1.3615 (1.3311) [0.0304]
$r_{B^3-H^b}$	1.3289 (1.3652) [-0.0363]	1.3611 (1.3652) [-0.0041]	1.3281 (1.3652) [-0.0371]	1.3610 (1.3652) [-0.0042]	1.3263 (1.3652) [-0.0389]
$r_{B^3-H^c}$	1.2753 (1.2910) [-0.0157]	1.2918 (1.2910) [0.0008]	1.2763 (1.2910) [-0.0147]	1.2917 (1.2910) [0.0007]	1.2757 (1.2910) [-0.0153]
$r_{B^4-H^c}$	1.4089 (1.3956) [0.0133]	1.3892 (1.3956) [-0.0064]	1.4054 (1.3956) [0.0098]	1.3870 (1.3956) [-0.0086]	1.4061 (1.3956) [0.0105]

* W represents the following bonds: C≡O, N≡CH, H−OH, H−NH$_2$ and H−OCH$_3$; W' represents the C−H (NCH and HOCH$_3$), O−H (H_2O), N−H (NH_3); Values of the monomers are given in parentheses and variations in bracket.

The values of the infrared stretch frequencies followed by their absorption intensities are organized in Table 2. The intermolecular systems studied in this work are formed by different types of interactions, wherein among them the bifurcated is the most active. Therefore, the identification of the new vibration modes becomes a hard task. Regardless, the values of 82.12 (**I**), 113.5 (**II**), 115.4 (**III**), 122.2 (**IV**) and 128.4 (**V**) cm^{-1} are in good agreement with the results of the hydrogen bond distances (**A**), such as is illustrated in the Fig. 2 and stated by the Eq. (1) and Eq. (2):

A: $u_{(Z \cdots H-X)} = -96.71 \, R_{(Z \cdots H-X)} + 372.89$, $r_A^2 = -0.91$ (1)

B: $u_{(H \cdots H-X)} = -49.79 \, R_{(H \cdots H-X)} + 206.74$, $r_B^2 = -0.96$ (2)
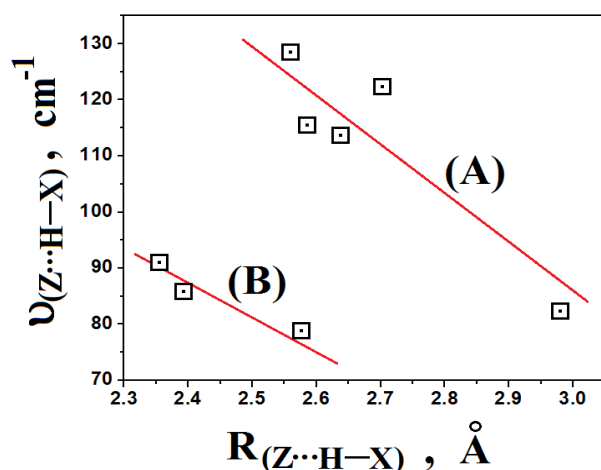

Fig. 2. Relationship between the values of the new vibrational modes and intermolecular distances. Z may be the charge density source for hydrogen bonds (**A**) or dihydrogen bonds (**B**).

Nevertheless, if the dihydrogen bonds (**B**) are taken into account, an intermolecular parallelism (**A**: it means hydrogen bonds) between structural and vibrational parameters may be formulated (Eq. 2). In a theoretical study [44], a comparative analysis between the interaction strength of the dihydrogen bonds and hydrogen bonds is discussed. Even though the relationship between structure and vibration is well correlated, a simpler and best interpretation (strength of **B** > strength of **A** only in terms of intermolecular distances) could be generated after examining the dihydrogen bonds. Note that, there is no systematic tendency concerning the strength between hydrogen bonds and dihydrogen bonds, e.g, the intermolecular distance in 2.6 Å brings (Fig. 3) two different types of new vibrational modes, which are located in 110-130 cm^{-1} for hydrogen bonds as well as in 80 cm^{-1} for dihydrogen bonds.

The Table 2 also lists the values of the frequency shifts and absorption intensity ratios. Corroborating with the specialized literature [45-46], here a direct relationship between the variations of the bond lengths and red and blue shifts of proton donors might be fairly obtained. Moreover, the values of the red shifts occur in the B^2−H^a bonds whereas in the B^3−H^c bonds are manifested the blue shift. Thereby, a correlation between the frequency shifts and variation of the bond lengths was generated, as such illustrated in the Fig. 3, and from this projection, a good linear coefficient (r^2) of 0.98 ruled by the Eq. (3) was obtained:

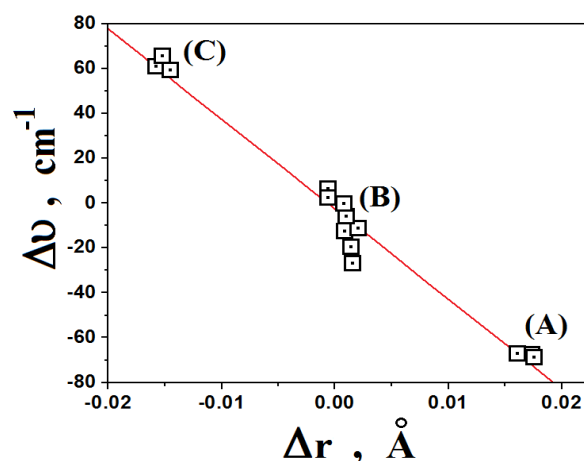$\Delta u = -4012.4 \, (\Delta r) - 2.59$, $r^2 = -0.98$ (3)

Fig. 3. Relationship between the values of the frequency shifts and variations of the bond lengths.

Regardless the magnitude of the red- and blue-shifts, Fig. 3 exposes them in three distinct groups. The red shifts (**A**) emerge justly in the B^2−H^a oscillators in full agreement with the variations of bond lengths, i.e., the B^2−H^a bonds in the **I**, **III** and **V** structures which undergo the most drastic lengthening, larger rather than the results of **II** and **IV**. In spite of this, in the complexes **II** and **IV** as well as **III** and **V**, all of them were spectroscopically characterized by moderate red shifts and large blue shifts (**B** and **C**) in both rW and B^3−H^c bonds.

On the contrary to that occurs in B^2−H^a bond, large blue shifts (**C**) are manifested in the B^3−H^c, although present exclusively in the **I**, **III** and **V** complexes. Once the hyperconjugation and hybridization play a decisive role in the interpretation of the hydrogen bonding, in particular its vibrational phenomenology, in line with this, the red shifts can be justified via hyperconjugation while the blue shifts shall be examined at light of hybridization, and both of them arise when weakly and strong bound complexes are formed [47]. Unfortunately, the results discussed here are in disagreement with this statement. Instead, the dihydrogen bond in **III**, **IV** and **V** were not taken into account because the very slight structural deformations and soft frequency shifts are attributed to the B^1−H^d bonds (see Fig. 1).

Interaction energies and charge transfer

The values of the interaction energies are presented in Table 3. Contrary to specialized literature [48-49], the values of BSSE outweigh the results of ΔZPE. Although the complexes B$_5$H$_{11}$···W encompass several interaction types, i.e., the hydrogen bonds and dihydrogen bonds, overestimated values of BSSE were expected [50]. By comparing with the results obtained at the MP4, QCISD(T), and CCSD(T) calculations, it is widely known that BSSE amounts are underestimated whether the MP2/aug-cc-pVDZ level of theory is executed [51]. Based on new vibration modes, it was demonstrated that **III**, **IV** and **V** are more strongly bound than **I** and **II**. However, the values of the intermolecular distances reveal that **III** and **V** are the stronger bonded complexes. With respect to the values of the energies corrected by BSSE and ΔZPE, the **II** and **V** complexes are the strongest bonded. Even so, the profile (Fig. 4) for the prediction of the interaction energy concerning the distances of the hydrogen bonds may be validated, and as can be seen, the correlation between the values of ΔE^C and R$_{(Z \cdots H-X)}$ is quite satisfactory.

$\Delta E^C = 19.42 \, R_{(Z \cdots H-X)} - 62.28$, $r^2 = 0.93$ (4)

Table 2. Vibration modes of the $B_5H_{11}\cdots CO$ (**I**), $B_5H_{11}\cdots NCH$ (**II**), $B_5H_{11}\cdots H_2O$ (**III**), $B_5H_{11}\cdots NH_3$ (**IV**) and $B_5H_{11}\cdots HOCH_3$ (**V**) complexes obtained at the MP2/aug-cc-pVDZ theoretical level.

Modes	Complexes				
	I	II	III	IV	V
$\upsilon_{(C\cdots H-B)}$	82.12	−	−	−	−
$I_{(C\cdots H-B)}$	0.78	−	−	−	−
$\upsilon_{(N\cdots H-B)}$	−	113.5	−	122.2	−
$I_{(N\cdots H-B)}$	−	6.16	−	1.43	−
$\upsilon_{(O\cdots H-B)}$	−	−	115.4	−	128.4
$I_{(O\cdots H-B)}$	−	−	12.3	−	2.42
$\upsilon_{(H\cdots H-B)}$	−	−	85.7	78.7	90.9
$I_{(H\cdots H-B)}$	−	−	5.05	2.78	0.58
υ_W	2076.6 (2071.9) [4.7]	1992.7 (1990.3) [2.4]	3784.7 (3804.1) [-19.4]	3615.66 (3633.11) [-17.45]	3814.17 (3840.8) [-26.66]
I_W	36.88 (34.4) [1.07]	0.19 (0.53) [0.35]	2.92 (4.14) [0.70]	7.06 (5.06) [1.3]	35.87 (34.34) [1.04]
$\upsilon_{B^2-H}{}^a$	2134.6 (2201.8) [-67.2]	2190.9 (2201.8) [-10.9]	2134.3 (2201.8) [-67.5]	2196.3 (2201.8) [-5.5]	2133.5 (2201.8) [-68.3]
$I_{B^2-H}{}^a$	60.3 (35.9) [1.7]	35.0 (35.9) [0.9]	57.7 (35.9) [1.6]	36.7 (35.9) [1.0]	57.4 (35.9) [1.6]
$\upsilon_{B^3-H}{}^c$	2195.9 (2134) [61.0]	2132.5 (2134) [-1.5]	2194 (2134) [60.0]	2133.5 (2134.0) [-0.5]	2196.3 (2134) [62.3]
$I_{B^3-H}{}^c$	35.33 (61.1) [0.57]	59.4 (61.1) [0.9]	34.7 (61.1) [0.56]	61.7 (61.1) [1.0]	39.1 (61.1) [0.6]

Values of υ and I are given in cm^{-1} and km mol^{-1}, respectively.

The interaction strength ruled by the charge distribution along the molecular surface is faithfully evidenced by a dipolar orientation, and naturally, by variations even though softly observed, after the formation of the complex [48-49]. According to values presented in Table 3, the reductions of all dipole moments are not in concordance with the strength of the hydrogen bonds. Together in Table 3, the values (ChElPG and NBO) of the charge transfers (ΔQ_W) and atomic charge variations (δQ) also are organized. The positive and negative variations for $\Delta Q^{ChElPG}{}_W$ represent donations and receiving of charge, respectively. In this context, the complexes **I**, **II** and **IV**, whose specific interaction sites contain carbon and nitrogen, all of them present losses of charge which, then, was transferred to B_5H_{11}. On the other hand, the results of -0.025 and -0.001 e.u. computed at the light of the ChElPG calculations accuse gains of charge in H_2O and $HOCH_3$ upon the formation of the **III** and **V** complexes.

Table 3. Values of the interaction energies (corrected by ΔZPE and BSSE), charge transfer and variation of atomic charges of the $B_5H_{11}\cdots CO$ (**I**), $B_5H_{11}\cdots NCH$ (**II**), $B_5H_{11}\cdots H_2O$ (**III**), $B_5H_{11}\cdots NH_3$ (**IV**) and $B_5H_{11}\cdots HOCH_3$ (**V**) complexes obtained at the MP2/aug-cc-pVDZ theoretical level.

Parameters	Complexes				
	I	II	III	IV	V
ΔE	-12.90	-21.90	-21.79	-23.40	-26.52
ΔZPE	2.59	2.85	5.00	5.00	3.82
BSSE	6.30	7.04	6.86	7.70	9.58
ΔE^C	-4.01	-12.01	-9.93	-10.70	-13.12
$\Delta\mu$	-0.105	-0.592	-0.693	-0.218	-0.944
ΔQ_W	0.063 (0.003)	0.020 (0.006)	-0.025 (0.006)	0.007 (0.001)	-0.001 (0.001)
δQ_C	0.130 (-0.016)	− (−)	− (−)	− (−)	− (−)
δQ_O	-0.067 (0.019)	− (−)	-0.049 (-0.018)	− (−)	0.020 (-0.012)
δQ_N	− (−)	0.008 (-0.038)	− (−)	0.125 (-0.014)	− (−)
$\delta Q_H{}^a$	-0.056 (-0.025)	0.011 (0.008)	-0.009 (-0.016)	0.032 (0.006)	-0.011 (-0.016)
$\delta Q_H{}^b$	-0.136 (0.007)	0.012 (0.015)	0.070 (0.019)	-0.003 (0.026)	0.079 (0.019)
$\delta Q_H{}^c$	-0.005 (0.029)	0.013 (0.008)	0.031 (0.037)	0.045 (0.006)	0.050 (0.026)

Values of ΔE, ΔZPE, BSSE and ΔE^C in kJ mol^{-1}; Values of $\Delta\mu$ in Debye (D); Values of Q in electronic units (e.u.); Values (ΔQ and δQ) of NBO in parentheses.

Once the interaction strength of these complexes shall also be ruled either by computing of the hydrogen bond lengths or spectroscopic analyses, a clear differentiation among **I** and **II** in comparison with **III**, **IV** and **V** has been established. Distinctly then, the greatest losses of charge are manifested in CO and NCH, in which the amounts determined via ChElPG computations are 0.063 and 0.020 e.u., respectively. This is amazing because these systems present long intermolecular distances and mainly, the lower vibrational modes and interactions energies, in particular, the complexes with carbon monoxide. Positive variations of atomic charge were determined through the NBO calculations. It means losses of charge concentration and thereby these results are unsatisfactory for unveiling the interaction strength through the charge transfer.

On the other hand, even though the NBO calculations fail in the description of the charge transfer, some of these atomic charge variations are systematic. Note that, the enhancement in the values of the atomic charges for all bridge-elements (carbon, nitrogen and oxygen) suggest a proton receptor behavior for CO, NCH, H_2O, NH_3 and $HOCH_3$. It is worthy to mention that this trend is not in line with the interaction energy. For instance, the δQ^C values of -0.016 and -0.012 e.u. are not correlated with the ΔE^C results of -4.01 and -13.12 $kJ.mol^{-1}$ of the **I** and **V** complexes, respectively. For the H^a, H^b and H^c elements, the interpretation of the interaction strength by means of the ChElPG results is inconsistent because the absence or concentration of charge between proton donors and bridge elements cannot be accurately measured. For δQH^b and δQH^c, however, an inverse donation of charge on the proton donors is reiterated by the positive NBO values.
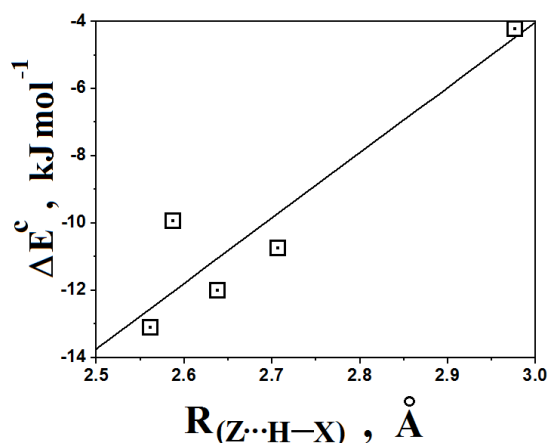

Fig. 4. Relationship between the values of the interaction energies and intermolecular distances

QTAIM study

The QTAIM [52-53] study was performed in order to evaluate the hydrogen bonds of the **I-V** complexes, wherein the results are listed in Table 4 and Table 5. Once these systems present a wide range of molecular sites for interacting with proton donors or even acceptor ones, the distinguishing of each hydrogen bond becomes unapproachable in this regard. The modeling of BPs and localization of BCPs are depicted in Fig. 5, by which the insight of several hydrogen bonds (bifurcate) on each complex can be definitely proven.

Table 4. QTAIM parameters of the hydrogen bonds of the **I**, **II** and **IV** complexes.

BCPs	Complexes		
	I	II	IV
$\rho_{(C\cdots H^a-B)}$	0.0043	—	—
$\nabla^2\rho_{(C\cdots H^a-B)}$	0.0154	—	—
$G_{(C\cdots H^a-B)}$	0.0028	—	—
$V_{(C\cdots H^a-B)}$	-0.0018	—	—
$-G/V_{(C\cdots H^a-B)}$	1.5555	—	—
$\rho_{(C\cdots H^b-B)}$	0.0050	—	—
$\nabla^2\rho_{(C\cdots H^b-B)}$	0.0175	—	—
$G_{(C\cdots H^b-B)}$	0.0033	—	—
$V_{(C\cdots H^b-B)}$	-0.0023	—	—
$-G/V_{(C\cdots H^b-B)}$	1.4347	—	—
$\rho_{(C\cdots H^e-B)}$	0.0038	—	—
$\nabla^2\rho_{(C\cdots H^e-B)}$	0.0127	—	—
$G_{(C\cdots H^e-B)}$	0.0023	—	—
$V_{(C\cdots H^e-B)}$	-0.0014	—	—
$-G/V_{(C\cdots H^e-B)}$	1.6428	—	—
$\rho_{(N\cdots H^d-B)}$	—	0.0038	0.0042
$\nabla^2\rho_{(N\cdots H^d-B)}$	—	0.0144	0.0175
$G_{(N\cdots H^d-B)}$	—	0.0027	0.0032
$V_{(N\cdots H^d-B)}$	—	-0.0018	-0.0021
$-G/V_{(N\cdots H^d-B)}$	—	1.5000	1.5238
$\rho_{(N\cdots H^b-B)}$	—	0.0079	0.0084
$\nabla^2\rho_{(N\cdots H^b-B)}$	—	0.0292	0.0275
$G_{(N\cdots H^b-B)}$	—	0.0060	0.0059
$V_{(N\cdots H^b-B)}$	—	-0.0048	-0.0049
$-G/U_{(N\cdots H^b-B)}$	—	1.2500	1.2040

Values of ρ and $\nabla^2\rho$ are given in $e.a_o^{-3}$ and $e.a_o^{-5}$, respectively; Values of G and V are given in electronic unites (e.u.).

Revisiting the evaluation of interaction strength, the values of the electronic density agree satisfactorily with the results of the hydrogen bond distances [54]. Although the efficient correlation between the values of the hydrogen bond distances and electronic densities can be further improved,

but individually each complex exhibits a satisfactory consonance regarding the interaction strength.

Since the preferential hydrogen bond of **III** is devoted to the shortest one, i.e., (C⋯H^a−B), ideally this one presents the higher charge density concentration with a value of 0.0043

e.a$_o^{-3}$. For the (N⋯H^b−B) hydrogen bond in **II** and **IV**, their shorter values of 2.6393 and 2.7043 Å are in inverse agreement with the charge densities of 0.0079 and 0.0084 e.a$_o^{-3}$, respectively. The complexes **III** and **V** are formed by the following hydrogen bonds (O⋯H^a−B) and (O⋯H^b−B), which are the shorter ones due to the values of 2.3944 and 2.5604 Å, respectively. It can be perceived that **V** exhibits a direct relationship between the results of R(O⋯H^b−B) and ρ(O⋯H^b−B), but in **III** the higher charge density was computed for O⋯H^b−B. The characterization of the hydrogen bonds as weak contacts being identified in the form of closed-shell interactions is ruled by the positive values of Laplacian [55].

Table 5. QTAIM parameters of the hydrogen bonds of the **III** and **V** complexes.

BCPs	Complexes	
	III	V
ρ$_{(O⋯H^a−B)}$	0.0066	−
∇^{2}ρ$_{(O⋯H^a−B)}$	0.0285	−
G$_{(O⋯H^a−B)}$	0.0058	−
V$_{(O⋯H^a−B)}$	-0.0044	−
-G/V$_{(O⋯H^a−B)}$	1.3181	−
ρ$_{(O⋯H^b−B)}$	0.0078	0.0094
∇^{2}ρ$_{(O⋯H^b−B)}$	0.0317	0.0353
G$_{(O⋯H^b−B)}$	0.0067	0.0077
V$_{(O⋯H^b−B)}$	-0.0054	-0.0065
-G/V$_{(O⋯H^b−B)}$	1.2407	1.1846
ρ$_{(O⋯H^e−B)}$	0.0039	0.0052
∇^{2}ρ$_{(O⋯H^e−B)}$	0.0169	0.0217
G$_{(O⋯H^e−B)}$	0.0031	0.0042
V$_{(O⋯H^e−B)}$	-0.0020	-0.0030
-G/V$_{(O⋯H^e−B)}$	1.5500	1.4100

Values of ρ and ∇^{2}ρ are given in e.a$_o^{-3}$ and e.a$_o^{-5}$, respectively; Values of G and V are given in electronic unites (e.u.).
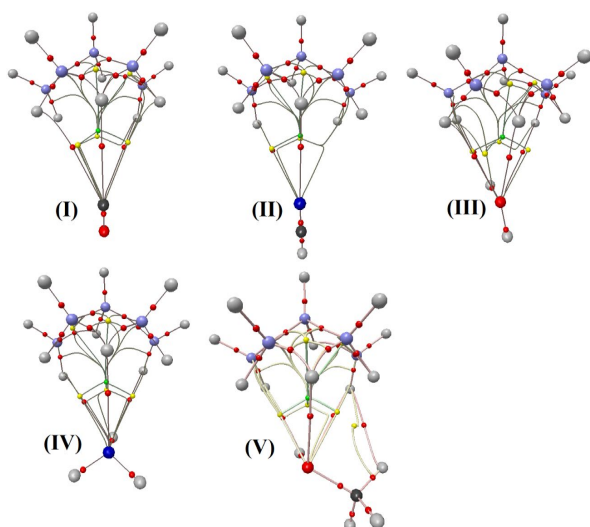

Fig. 5. BCPs and BPs computed by the QTAIM calculations.

Nevertheless, the qualitative prediction of the interaction strength can be stressed through the contributions of both descriptors G and V, especially through the ratio between them [56]. The −G/V ratio classifies the interaction strength as i) noncovalent if −G/V > 1; ii) partially covalent if 0.5 < −G/V < 1.0; and iii) totally covalent if −G/V < 0.5 [57]. In according with the values of −G/U listed in Tables 4 and 5, the hydrogen bonds of the **I**-**V** complexes are non-covalent with a satisfactory relationship with the interaction energy (see Fig. 6):

$$\Delta E^C = 32.58 \, (-G/V) - 51.60 \quad , \quad r^2 = 0.93 \qquad (5)$$

In comparison with the B$_5$H$_{11}$⋯O$_2$ and B$_5$H$_{11}$⋯N$_2$ complexes [44], even though all I-V systems are more strongly bound, the interaction strength unveiled by means of the relationship of -G/V points out a less covalent character. Besides hydrogen bonds, the Table 6 organizes the values of the QTAIM parameters for the dihydrogen bonds of the **III**, **IV** and **V** complexes. Once again, the relationship between the distance and charge density may be established. The dihydrogen bond labeled as H⋯H^d−B in **V** is the shortest due to the length of 2.3563 Å followed by the higher charge density of 0.0056 e.a$_o^{-3}$.
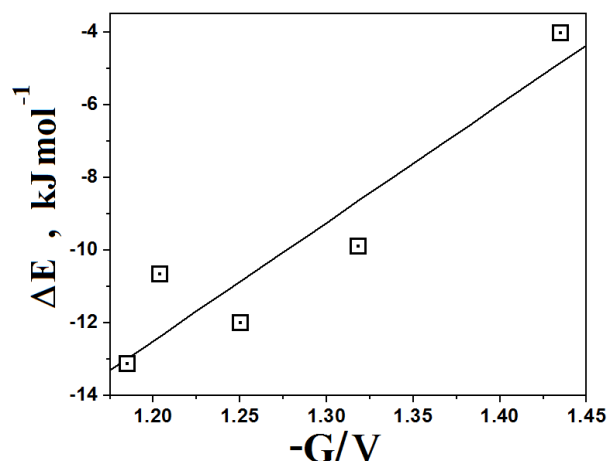

Fig. 6. Relationship between the values of the interaction energies and ratios of kinetic and potential energy densities.

For the others dihydrogen bonds, the length values of 2.3944 (**III**) and 2.5775 Å (**IV**) correlated well with the electronic densities of 0.0049 and 0.0043 e.a$_o^{-3}$, respectively. In addition, the positive results of Laplacian reveal a non-covalent character for these dihydrogen bonds. Still regarding the −G/V ratio, which has been used for predicting the covalent character, surely this is only a qualitative parameter because the weaker interactions in **II**, e.g., -G/V(N⋯H^b−B), the value of 1.2500 Å is moderately distant to the threshold to be considered as partially covalent.

Table 6. QTAIM parameters of the H⋯H−B dihydrogen bonds of the **III**, **IV** and **V** complexes.

BCPs	Complexes		
	III	IV	V
ρ$_{(H⋯H^d−B)}$	0.0049	−	0.0056
∇^{2}ρ$_{(H⋯H^d−B)}$	0.0219	−	0.0238
G$_{(H⋯H^d−B)}$	0.0041	−	0.0046
U$_{(H⋯H^d−B)}$	-0.0029	−	-0.0032
-G/V$_{(H⋯H^d−B)}$	1.4398	−	1.4070
ρ$_{(H⋯H^e−B)}$	−	0.0042	−
∇^{2}ρ$_{(H⋯H^e−B)}$	−	0.0177	−
G$_{(H⋯H^e−B)}$	−	0.0032	−
V$_{(H⋯H^e−B)}$	−	-0.0021	−
-G/V$_{(H⋯H^e−B)}$	−	1.5470	−

Values of ρ and ∇^{2}ρ in e.a$_o^{-3}$ and e.a$_o^{-5}$, respectively; Values of G and V are given in electronic unites (e.u.).

4. Conclusions

The theoretical study of the B$_5$H$_{11}$⋯CO, B$_5$H$_{11}$⋯NCH, B$_5$H$_{11}$⋯NH$_3$, B$_5$H$_{11}$⋯H$_2$O and B$_5$H$_{11}$⋯HOCH$_3$ complexes was a

challenging investigation due to the high complexity of the *arachno*-pentaborane (11) molecule. In spite the non-covalent intermolecular condition of these systems, the results showed a certain systematic tendency of the interaction strength. Regardless, the profile of interaction strength and mainly the capability of the B_5H_{11} behaving as a host-guest molecule, two class of systems were recognized, e.g., those with CO and H_2O forming the weakest bound complexes (weakening of the C≡O bond) and the others with NCH, NH_3 and $HOCH_3$ (lengthening in the H−O and H−N bonds) as being the stronger ones. The results of the frequencies shifted to red and blue are in line with the profiles of the structural tendencies. Due to the large number of intermolecular interactions, hydrogen bonds and dihydrogen bonds, which are the weaker and stronger ones respectively under the structural point of view, the interaction energy values could not be distributed in weighted way, although a direct relationship with the values of the shortest hydrogen bonds was declared**.** The determination of the charge transfer amounts via both ChElPG and NBO calculations as well as the variations of dipole moment, all these ones belong to a set of unapproachable parameters for describing the interaction strength of the $B_5H_{11}\cdots CO$, $B_5H_{11}\cdots NCH$, $B_5H_{11}\cdots NH_3$, $B_5H_{11}\cdots H_2O$ and $B_5H_{11}\cdots HOCH_3$ complexes. Moreover, the non-covalent character was demonstrated by means of the QTAIM calculations through the comparison between the kinetic and potential energy densities, which are in good concordance with the interaction energy computed at light of the supermolecule approach.

References and Notes

[1] Iribarren, I.; Sánchez-Sanz, G.; Alkorta, I.; Elguero, J.; Trujillo, C. *J. Phys. Chem. A* **2021**, *125*, 4741. **[Crossref]**

[2] Schneider, H.-J. *Phys. Org. Chem*. **2022**, *35*, e4340. **[Crossref]**

[3] Fabbrizzi, L. *ChemPlusChem*, **2022**, *87*, e202100243. **[Crossref]**

[4] Del Bene, J.; Alkorta, I.; Elguero, J. *Molecules*, **2020**, *25*, 2846. **[Crossref]**

[5] Aarabi, M.; Gholami, S.; Grabowski, S. J. *Molecules*, **2021**, *26*, 6939. **[Crossref]**

[6] Hammami, F.; Issaoui, N. *Front. Phys.* **2022**, *10*, 1. **[Crossref]**

[7] Tulsiyan, K. D.; Jena, S.; Dutta, J.; Biswal, H. S. *Phys. Chem. Chem. Phys*. **2022**, *24*, 17185. **[Crossref]**

[8] Wysokiński, R.; Zierkiewicz, W.; Michalczyk, M.; Maris, T.; Scheiner, S. *Molecules*, **2022**, *27*, 2144. **[Crossref]**

[9] Alkorta, I.; Elguero, J.; Frontera, A. *Crystals* **2020**, *10*, 180. **[Crossref]**

[10] Karas, L. J.; Wu, C.-H.; Das, R.; Wu, J. I.-C. *WIREs Comput. Mol. Sci*. **2020**, *10*, e1477. **[Crossref]**

[11] Nekoei, A.-R.; Vatanparasta, M. *Phys. Chem. Chem. Phys.* **2019**, *21*, 623. **[Crossref]**

[12] Ghosh, S.; Wategaonkar, S. *J. Indian Inst. Sci.* **2020**, *100*, 101. **[Crossref]**

[13] Jin, P.-B.; Luo, Q.-C.; Zhai, Y.-Q.; Wang, Y.-D.; Ma, Y.; Tian, L.; Zhang, X.; Ke, C.; Zhang, X.-F.; Lv, Y.; Zheng, Y.-Z. *iScience* **2021**, *24*, 102760. **[Crossref]**

[14] Saha, B.; Chandel, D.; Rath, S.P. *Inorg. Chem.* **2022**, *61*, 2154. **[Crossref]**

[15] Zhao, D.; He, X.; Li, M.; Wang, B.; Guo, C.; Rong, C.; Chattaraj, P. K.; Liu, S. *Phys. Chem. Chem. Phys*. **2021**, *23*, 24118. **[Crossref]**

[16] Vedejs, E. *Science* **1980**, *207*, 42. **[Crossref]**

[17] Lipscomb, W. N. *Science* **1977**, *196*, 1047. **[Crossref]**

[18] Zabardasti, A.; Kakanejadifard, A.; Hoseini, A. A.; Solimannejad, M. *Dalton Trans*. **2010**, *39*, 5918. **[Crossref]**

[19] Taylor, R. *Acta Crystal. B* **2017**, *73*, 474. **[Crossref]**

[20] Crabtree, R. H. *Chem. Rev.* **2016**, *116*, 8750. **[Crossref]**

[21] Chen, X.; Bai, Y.-K.; Zhao, C.-Z.; Shen, X.; Zhang, Q. *Angew. Chem. Int. Ed.* **2020**, *59*, 11192. **[Crossref]**

[22] Kara, T.; Scheiner, S. *J. Chem. Phys.* **2003**, *119*, 1473. **[Crossref]**

[23] Ingram, D. J.; Headen, T. F.; Skipper, N. T.; Callear, S. K.; Billing, M.; Sella, A. *Phys. Chem. Chem. Phys.* **2018**, *20*, 12200. **[Crossref]**

[24] Zabardasti, A.; Arabpour, M.; Zare, N. *Comput. Theor. Chem.* **2013**, *1008*, 27. **[Crossref]**

[25] Zabardasti, A.; Goudarziafshar, H.; Salehnassaj, M.; Oliveira, B. G. *J. Mol. Model*. **2014**, *20*, 2403. **[Crossref]**

[26] Jabłoński, M. *Molecules* **2020**, *25*, 5512. **[Crossref]**

[27] Atalla, V.; Yoon, M.; Caruso, F.; Rinke, P.; Scheffler, M. *Phys. Rev. B*. **2013**, *88*, 165122. **[Crossref]**

[28] Oliveira, B. G.; Araújo, R. C. M. U.; Carvalho, A. B.; Ramos, M. N. *J. Mol. Model*. **2009**, *15*, 421. **[Crossref]**

[29] Wang, L.; Zhang, T.; He, H.; Zhang, J. *RSC Adv*. **2013**, *3*, 21949. **[Crossref]**

[30] Oliveira, B. G. *Rev. Bras. Ens. Fís*. **2020**, *42*, e20190061. **[Crossref]**

[31] Bader, R. F. W. *Chem. Rev*. **1991**, *91*, 893. **[Crossref]**

[32] Oliveira, B. G. *Phys. Chem. Chem. Phys*. **2013**, *15*, 37. **[Crossref]**

[33] Oliveira, B. G.; Araújo, R. C. M. U.; Carvalho, A. B.; Ramos, M. N. *Spectrochim. Acta A*. **2015**, *145*, 580. **[Crossref]**

[34] Oliveira, B. G.; Araújo, R. C. M. U.; Carvalho, A. B.; Ramos, M. N. *Struct. Chem*. **2009**, *20*, 663. **[Crossref]**

[35] Oliveira, B. G.; Araújo, R. C. M. U.; Carvalho, A. B.; Ramos, M. N. *Spectrochim. Acta A*. **2010**, *75*, 563. **[Crossref]**

[36] Frisch, M. J.; Trucks, G. W.; Schlegel, H. B.; Scuseria, G. E.; Robb, M. A.; Cheeseman, J. R.; Scalmani, G.; Barone, V.; Mennucci, B.; Petersson, G. A.; Nakatsuji, H.; Caricato, M.; Li, X.; Hratchian, H. P.; Izmaylov, A. F.; Bloino, J.; Zheng, G.; Sonnenberg, J. L.; Hada, M.; Ehara, M.; Toyota, K.; Fukuda, R.; Hasegawa, J.; Ishida, M.; Nakajima, T.; Honda, Y.; Kitao, O.; Nakai, H.; Vreven, T.; Montgomery, Jr. J. A.; Peralta, J. E.; Ogliaro, F.; Bearpark, M.; Heyd, J. J.; Brothers, E.; Kudin, K. N.; Staroverov, V. N.; Kobayashi, R.; Normand, J.; Raghavachari, K.; Rendell, A.; Burant, J. C.; Iyengar, S. S.; Tomasi, J.; Cossi, M.; Rega, N.; Millam, J. M.; Klene, M.; Knox, J. E.; Cross, J. B.; Bakken, V.; Adamo, C.; Jaramillo, J.; Gomperts, R.; Stratmann, R. E.; Yazyev, O.; Austin, A. J.; Cammi, R.; Pomelli, C.; Ochterski, J. W.; Martin, R. L.; Morokuma, K.; Zakrzewski, V. G.; Voth, G. A.; Salvador, P.; Dannenberg, J. J.; Dapprich, S.; Daniels, A. D.; Farkas, O.; Foresman, J. B.; Ortiz, J. V.; Cioslowski, J.; Fox, D. J.; Gaussian, Inc., Wallingford CT, Gaussian 09, Revision A. 02, 2009.

[37] Anick, D. J. *J. Phys. Chem*. **2005**, *109*, 5596. **[Crossref]**

[38] Brauer, B.; Kesharwani, M. K.; Martin, J. M. L. *J. Chem. Theor. Comput*. **2014**, *10*, 3791. **[Crossref]**

[39] Biegler-König, F.; Schönbohm, J. *J. Comput. Chem*. **2002**, *23*, 1489. **[Crossref]**

[40] Padiyar, G. S.; Seshadri, T. P. *Nuc. Nuc*. **1996**, *15*, 857. **[Crossref]**

[41] Korona, T.; Dodziuk, H. *J. Chem. Theor. Comput*. **2011**, *7*, 1476. **[Crossref]**

[42] Oliveira, B. G. *Struct. Chem*. **2014**, *25*, 745. **[Crossref]**

[43] Oliveira, B. G. *Quim. Nova* **2015**, *38*, 1313. **[Crossref]**

[44] Oliveira, B. G.; Zabardasti, A.; Goudarziafshar, H.; Salehnassaj, M. *J. Mol. Model*. **2015**, *21*, 77. **[Crossref]**

[45] Oliveira, B. G. *Quim. Nova* **2016**, *39*, 320. **[Crossref]**

[46] Oliveira, B. G. *Chem. Phys*. **2014**, *443*, 67. **[Crossref]**

[47] Grabowski, S. J. *J. Phys. Chem. A* **2011**, *115*, 12789. **[Crossref]**

[48] Oliveira, B. G.; Leite, L. F. C. C. *J. Mol. Struct. (THEOCHEM)* **2009**, *915*, 38. **[Crossref]**

[49] Oliveira, B. G.; Araújo, R. C. M. U.; Carvalho, A. B; Ramos, M. N. *J. Mol. Model*. **2011**, *17*, 2847. **[Crossref]**

[50] Orimoto, Y.; Yamamoto, R.; Xie, P.; Liu, K.; Imamura, A.; Aoki Y. *J. Chem. Phys*. **2015**, *142*, 104111. **[Crossref]**

[51] Van Mourik, T.; Wilson, A. K.; Peterson, K. A.; Woon, D. E.; Dunning Jr., T. H. *Adv. Quantum Chem*. **1998**, 31, 105. **[Crossref]**

[52] Pandiyan, B. V.; Kolandaivel, P.; Deepa, P. *Mol. Phys*. **2014**, *112*, 1609. **[Crossref]**

[53] Oliveira, B. G.; Araújo, R. C. M. U. *Can. J. Chem*. **2012**, *90*, 368. **[Crossref]**

[54] Santos, G. F. N.; Carvalho, L. C.; Oliveira, D. A. S.; Rego, D. G.; Bueno, M. A.; Oliveira, B. G. *J. Phys. Org. Chem*. **2020**, *33*, e4098. **[Crossref]**

[55] Oliveira, B. G. *Comp. Rend. Chim*. **2014**, *17*, 1041. **[Crossref]**

[56] Oliveira, B. G. *Comp. Rend. Chim*. **2016**, *19*, 995. **[Crossref]**

[57] Grabowski, S. J. *Chem. Rev*. **2011**, *111*, 2597. **[Crossref]**

How to cite this article